JOURNAL OF MATERIALS SCIENCE 26 (1991) 2645–2650

Effect of microstructure on mechanical properties in 0.5 carbon–steel processed by high temperature thermomechanical treatment

YOSHIYUKI TOMITA
Department of Metallurgical Engineering, College of Engineering, University of Osaka Prefecture, 4-804 Mozu-Umemachi, Sakai, Osaka 591, Japan

The effect of microstructure on the slow bending stress and fracture energy in 0.5C–steel processed by high temperature thermomechanical treatment (processed by forging) (HTMT) was studied to understand which microstructural factors contribute to the strength and toughness of a HTMT steel. Significant improvement was achieved in the slow bending fracture energy, with moderate increase in the slow bending stress when the steel was deformed by 50% at 1473K followed by direct water quenching and subsequent tempering at 453 K. When the steel was deformed by 50% reduction at 1173 K followed by direct water quenching and subsequent tempering at 423 K, the slow bending stress significantly increased though the increase in the fracture energy was not as great as that of the 1473 K forged steel. However, an abrupt reduction occurred in the fracture energy above suitable tempering temperatures, so above these temperatures, there was little difference between the properties of the HTMT and conventional heat-treated steels. Microstructural factors contributing to the mechanical properties are discussed in terms of thin-foil transmission electron microscopy, non-isothermal dilatometry, and X-ray measurements.

1. Introduction

In recent years, the use of high strength, low alloy steels has increased for tough structural application. However, conventional heat treatment cannot always meet current engineering requirements because of their lack of toughness in severe environments.

The realm of HTMT appears very attractive for high strength applications. This process involves deformation at temperatures above the A_{c_3} (stable austenite region) prior to quenching to form martensite. Therefore, this technique has been applied to low and medium alloy steels whose *S*-curve approaches the left. In addition, there is a great advantage that ductility and toughness are greatly improved without sacrificing the strength; therefore, one should consider HTMT as one of the potential approaches for developing the mechanical properties in severe environments. Research has been directed toward improved mechanical properties through HTMT processing [1, 2]; however, there are few systematic studies of microstructural factors contributing to the mechanical properties of a HTMT steel. Therefore, it would be useful to study a correlation of the mechanical properties and microstructure in a HTMT steel for commercial applications and to report on the factors contributing to the mechanical properties as a research problem.

In the present work, the effect of microstructure on the slow bending stress and fracture energy in 0.5C–steel processed by HTMT was investigated with the aim of clarifying the main microstructural factors contributing to the mechanical properties of a HTMT steel.

2. Experimental procedure

Commercial 0.5C–steel, which was air-melted and vacuum-degassed, was used in this investigation. The chemical composition and A_{r_1}, A_{r_3} and M_s temperatures are given in Table I. The steel was received as 80 mm diameter hot-rolled bars stock. Test steels were received from the bars to 15 mm × 15 mm × 120 mm. Each was fully annealed.

The thermal and thermomechanical treatment schedules for test steels are given in Table II. Austenitization was conducted using an argon atmosphere furnace. Forging was made by a blow at a strain rate of 80 $N s^{-1}$ using an air-hammer at maximum capacity of 1.47 MN. The time interval between the upsetting and quenching for the specimens was about 2 s. An oil was used for tempers at 533 K and below and a lead-tin bath for tempers above 533 K.

The mechanical properties were determined using three-point slow bending tests. The slow bending tests (length of span = 50 mm) were made using specimens with dimensions of 4 mm × 20 mm × 80 mm on an Instron machine at a crosshead speed of 0.01 mm s^{-1} at room temperature (293 K). The slow bending fracture energy was estimated by the area under

0022–2461/91 $03.00 + .12

TABLE I Chemical composition of steel used (wt %) A_{r_1}, A_{r_3} and M_s were determined by standard dilatometry: the values are, respectively, 994, 1026, and 601 K.

C	Si	Mn	P	S
0.50	0.31	0.70	0.021	0.012

TABLE II Thermal and thermomechanical treatment schedules.

Designation	Thermal and thermomechanical treatments
1173 K–HTMT	Austenitize at 1173 K (7.2 ks), 50% hot-forge, water quench
1473 K–HTMT	Austenitize at 1473 K (7.2 ks), 50% hot-forge, water quench
Conventional heat treatment (CHT)	Austenitize at 1473 K (7.2 ks), 50% hot-forge, air cool, re-austenitize at 1133 K (7.2 ks), water quench

stress–deflection curve which was measured by a planimeter.

Microstructure of the specimens was examined using thin-foil transmission electron microscopy (TEM). Thin foils were prepared by grinding to a 0.1 mm thickness, then chemically thinning in a mixed solution of hydrofluoric acid and hydrogen peroxide, followed by electropolishing in a mixed solution of phosphoric and chromic acids. Retained austenite contents were determined by the Miller technique [3] of rotating and tilting the sample surface to an incident beam using MoK_α radiation. A scanning speed of 0.0003 deg s^{-1} was generally used for weak austenite diffraction, compared with the through scanning speed normally employed for martensitic peaks of 0.003 deg s^{-1}. The combination of peaks chosen for the analysis was (2 1 1)α, (2 2 0)γ, and (3 1 1)γ. Tempering kinetics were analysed using non-isothermal dilatometry [4]. The dilatometry was performed by continuous heating under vacuum at a controlled rate of 0.008 K s^{-1}. The test specimens were 4 mm in diameter and 80 $\pm$ 0.25 mm in length. The activation energy, E, was determined by Equation 1

$$E = -nRT_i^2 C_i^{n-1} (dC/dT)_i / C_i^n \quad (1)$$

where n and R are, respectively, the order of reaction and the gas constant, and T_i, C_i and $(dC/dT)_i$ are the temperature, length fraction of remaining reactant and slope of a tangent at the inflection point of the curves plotted as the length fraction of remaining reactant against temperature, respectively.

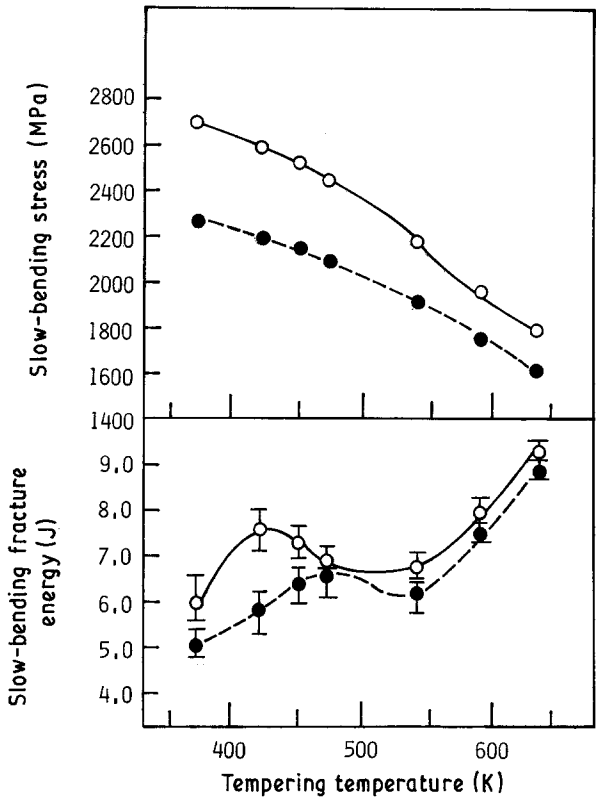

Figure 1 Effect of tempering temperature on slow bending stress and fracture energy of (○) 1173K–HTMT and (●) CHT steels.

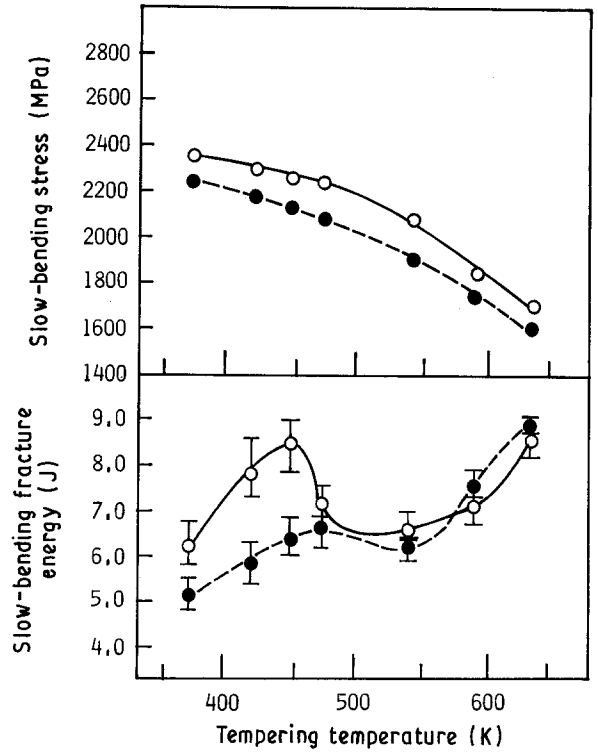

Figure 2 Effect of tempering temperature on slow bending stress and fracture energy of (○) 1473K–HTMT and (●) CHT steels.

3. Results

3.1 Mechanical tests

Figs 1 and 2 show the effect of tempering temperature on slow bending stress and slow bending fracture energy of the HTMT and conventionally heat-treated (CHT) steels. The slow bending stress of the 1173 K–HTMT steel, compared with that of the CHT steel, significantly increased the slow bending stress for temper of 423 K owing to the moderate increase in slow bending fracture energy (Fig. 1). The significant improvement was achieved in the slow bending fracture energy for temper at 453 K, with a moderate increase in slow bending stress by processing 1473K–HTMT (Fig. 2). There was an abrupt reduction, however, in the slow bending fracture energy of the HTMT steels above suitable tempering temper-

atures, so that above these temperatures there was little difference in the properties between the HTMT and CHT steels.

3.2 Microstructure

In order to elucidate the effect of microstructure and improved mechanical properties of HTMT steel, TEM observations were made of HTMT steels tempered at temperatures showing the better mechanical properties, i.e., designated at 1173 K–HTMT–423 K Tempered and 1473–HTMT–453 K Tempered steels. Comparisons were made with the CHT steel tempered at 473 K (designated at CHT–473 K Tempered steel). Typical results are shown in Fig. 3. The TEM observations revealed that the microstructure of the 1173 K–HTMT–423 K Tempered and 1473 K–HTMT–453 K Tempered steels consisted predominantly of a ellipsoidal subcell structure, whereas, the CHT–473 K Tempered steel possessed lath martensitic morphology. The TEM observations also revealed that a decrease in twin density and a slight coarsening of subcells size was observed for 1473 K–HTMT–453 K Tempered steel. The TEM observations were made of the HTMT and CHT steels tempered at 533 K, i.e., designated 1173 K–HTMT–433 K Tempered, 1473 K–HTMT–533 K Tempered and CHT–533 K Tempered steels, in order to reveal correlation of microstructure and an abrupt loss in the slow bending fracture energy. The typical results are shown in Fig. 4. The TEM observations revealed, however, that for the 1173 K–HTMT–533 K Tempered and 1473 K–HTMT–533 K Tempered steels, fine carbide precipitation was found on dislocations in the subcell independent of forging temperature, whereas, for the CHT–533 K Tempered steel, long elongated carbides along prior austenite grain boundaries as well as interlath rod carbides were observed. Indexing of the ring diffraction pattern of the carbides showed that a majority of the carbides could be identified as Fe_3C.

3.3 Non-isothermal dilatometry

The foregoing TEM observations suggested that an abrupt reduction in the fracture energy was correlated with fine carbide precipitation in the subcell during tempering. In order to further investigate the carbide

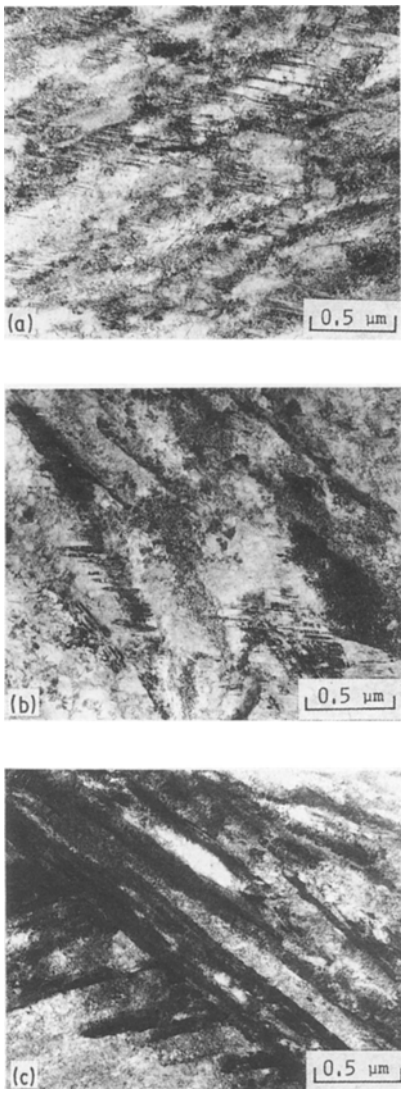

Figure 3 TEM micrographs of HTMT and CHT steels tempered at temperatures showing better mechanical properties; (a) 1173 K–HTMT–423 K Tempered steel; (b) 1473 K–HTMT–453 K Tempered steel; (c) CHT–473 K Tempered steel.

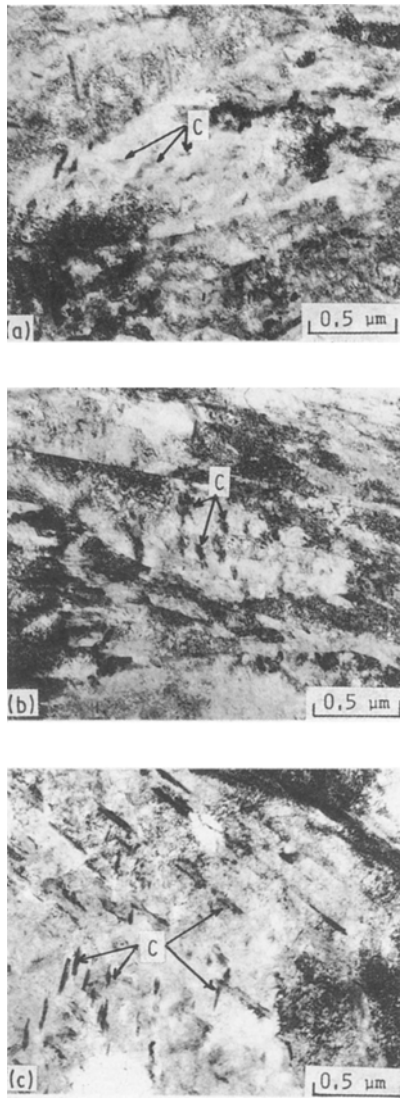

Figure 4 TEM micrographs of HTMT and CHT steels tempered at 533 K; (a) 1173 K–HTMT–533 K Tempered steel; (b) 1473K–HTMT–533 K Tempered steel; (b) CHT–533 K Tempered steel. C indicates carbide.

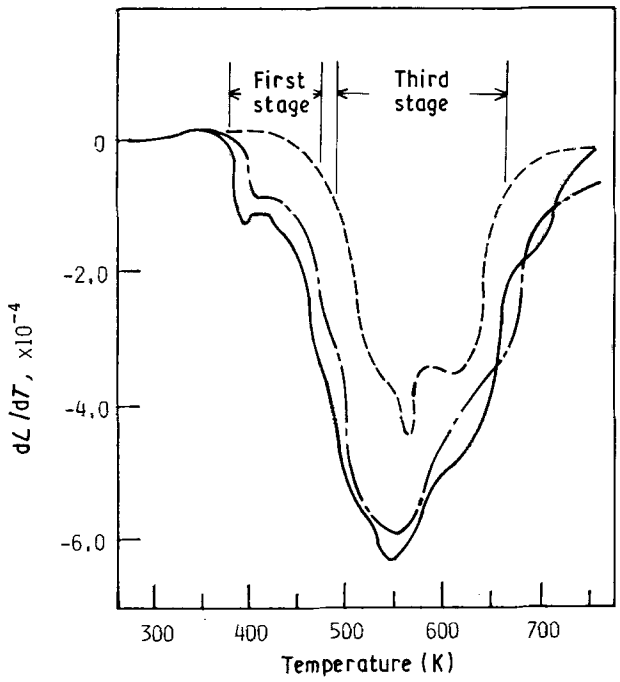

Figure 5 Temperature derivatives dL/dT versus tempering temperature in dilation curves for (—) 1173 K–HTMT, (– – –) 1473 K–HTMT and (– – –) CHT steels (heating rate = 0.008 K s^{-1}).

precipitation behaviour of the HTMT steels during tempering, non-isothermal dilatometry was conducted. Fig. 5 shows a comparison of the temperature derivative of the dilation curves between the HTMT and CHT steels. The dilatometry revealed that temperatures at which the first and third stages begin, significantly decreased for the HTMT steels as compared with the CHT steel at the same temperature levels. These temperatures somewhat increased as forging temperature increased. So, in order to estimate this quantitatively, the apparent activation energy values of the third stage of tempering were evaluated using Equation 1. The results are shown in Table III. As seen from this table, the apparent activation energy of the third stage in tempering significantly decreased by processing HTMT. That is to say, the activation energy values of the 1173 K–HTMT and 1473 K–HTMT steels were, respectively, 57.06 and 61.20 kj mol^{-1}, whereas, for that of the CHT steel was 83.17 kj mol^{-1}.

4. Discussion

4.1 Microstructural factors controlling strength and toughness of HTMT steel

Any suggested mechanism for mechanical properties of HTMT steels must be greatly influenced by the resultant microstructural changes; therefore, it is worthwhile to summarize the foregoing microstructural results. Summarizing the results, the marked microstructural changes which occurred by processing HTMT fall into two categories. One is the development of subcell structure for tempers showing the better mechanical properties and the other is fine carbide precipitation on dislocations in the subcell for tempers above suitable tempering temperature, which has a detrimental effect on fracture toughness. Discussion is now focused on these categories.

It has been recognized by many investigators [4–9] that subcell structure resulted in increased strength, the strength increasing with decreasing subcell size according to the Hall–Pettch relationship [5–9]. However, the problem to be solved is how a subcell contributes to improved toughness. Although the subcell effects on toughness are not as well understood as those on strength, there have been some evidence that subcell structure introduced by the thermal and thermomechanical treatments has a favourable effect on toughness. Morrison and Miller [10] have shown that reduction in the area of ultrafine-grained steel increases with decreasing subcell size and this could be a result of the cell walls acting as barriers to crack growth preceding final fracture. Irani [11] has demonstrated in a study of the isoforming of a Fe–Cr alloy steel that fine subcell introduced through isoforming, significantly contributes to improved impact toughness as well as strength of the steel. Araki and coworkers [12, 13] have shown that fine subcell is observed in the martensitic structure of ausformed 5Cr–Mo, 5Ni–Mo, and 5Mo steels and that subcell has a beneficial effect on toughness. They suggested that this desirable effect can be attributed to the higher stress concentration at a crack tip, being effectively relieved by the movement of the dislocation in the subcell. Thus, the present author believes that subcell structure contributes to the improved strength and toughness, acting as a wall of moving dislocations, but giving an extensive moving plastic zone.

Another important fact is that fine carbide precipitation during tempering HTMT steel is consistent with the observed abrupt reduction in the slow bending fracture energy. The present author believes that this can be explained by the Tayler model [14] giving rise to localization of plastic flow at the crack tip. Tayler assumed that if the average distance a dislocation moves before it stops is L and if the density of dislocations after a given deformation is D, then the plastic strain ε is given by DLb, where b is the Burgers vector. Therefore, if fine carbides precipitate on the dislocations, as seen in the present results, the plastic

TABLE III Activation energy values of the third stage in tempering of HTMT and CHT steels calculated using Equation 1 (heating = 0.008 K s^{-1})[a]

Designation of steel	T_i (K)	C_i	$(dC/dT)_i$ (K^{-1})	Activation energy, E (kj mol^{-1})
1173 K–HTMT steel	505	0.39	-1.05×10^{-2}	57.06
1473 K–HTMT steel	523	0.39	-1.04×10^{-2}	61.20
CHT steel	575	0.37	-1.12×10^{-2}	83.17

[a] $n = 1$, R = 8.31 j mol^{-1} K^{-1}

strain is greatly suppressed by precipitate locking. Furthermore, when the intersections and jog through the precipitate locked dislocations occur ahead of the current crack, localization of plastic flow will be produced at the crack tip. The findings that the reduction in toughness is associated with the interaction between precipitates and dislocations within grains has also been reported by other investigators. Banerjee [15] has demonstrated that the abrupt reduction in toughness in the tempered martensite embrittlement range of high strength steels (including AISI 4340, H11, and 422 stainless steels) can be explained in terms of a unified mechanistic concept involving precipitation locking of dislocation intersections and jogs, with high values of dislocation density during carbide resolution and re-precipitation steps.

4.2 Considerations of other microstructural factors

It may be seen from the foregoing data together with the above arguments that the microstructural factors contributing to the strength and toughness of HTMT steel are subcell structures introduced in austenite by processing HTMT and inherited by martensite, and fine carbide precipitation on dislocations in the subcell during tempering. However, there have been hitherto described microstructural factors to explain the mechanical properties. Discussion will centre on the microstructural factors. It has been recognized by many investigations that retained austenite greatly influences toughness in these types of low alloy steels [16–18]; therefore, X-ray measurements were made of specimens processed by HTMT and CHT steels. X-ray measurements revealed that retained austenite contents (3.2–3.6 vol %) are somewhat decreased as compared with those (2.6–2.8 vol %) of the CHT steel, although the difference is not extreme. This contrasts with the fact that the retained austenite contents following thermomechanical treatment usually increase. This could be due to the fact that residual stress produced by forging promoted martensitic transformation during quenching [19, 20]. Thus, it appears that retained austenite does not influence the toughness of HTMT steel. It has been reported that microtwinning influences strength and toughness of low alloy steels [21, 22]. As seen from the foregoing data, twin density increased as deformation temperature decreased. This change of twin density is consistent with the fact that the slow bending stress increased and the slow bending fracture energy decreased as deformation temperature decreased. However, it appears that although microtwinning influences the mechanical properties of HTMT steel, it is not a major microstructural factor now. There have been some investigations (for example, it is reviewed in [1]) that fine carbide precipitation occurs during HTMT in spite of the fact that the process is performed at temperatures where the solution of carbon in austenite is thermodynamically stable. Therefore, fine carbide precipitation in this investigation may occur during HTMT; however, as seen from the foregoing microstructural results, the carbide precipitation during HTMT appears to be unlikely to occur. In addition, if the carbide precipitation had occurred during HTMT, the carbon content of martensite will decrease and hence, temperatures, in which the first and third stage of tempering begin, will increase. This is contrary to the results shown in Fig. 5. Thus, it appears that the observed fine carbide precipitation occurred during tempering.

5. Conclusions

The effect of microstructure on the slow bending stress and fracture energy in 0.5C–steel processed by high temperature thermomechanical treatment (HTMT) (processed by forging) were studied to clarify the microstructural factors which contribute to the strength and toughness of HTMT steels.

1. A significant improvement was achieved in the slow bending fracture energy, coupling moderate increase in the slow bending stress when the steel was deformed by 50% reduction at 1473 K followed by direct water quenching and subsequent tempering at 453 K.

2. When the steel was deformed by 50% reduction at 1173 K followed by direct water quenching and subsequent tempering at 423 K, the slow bending stress significantly increased, while an advantage in the fracture energy was not as great as that achieved by 1473 K forging.

3. There was an abrupt reduction in the slow bending fracture energy of HTMT steels above suitable tempering temperatures so that above these temperatures there was little difference in the property of the HTMT and conventional heat-treated steel.

4. The beneficial effect on strength and toughness for the suitable tempering temperature is attributed to the fine subcell structure introduced in austenite during HTMT and inherited by martensite. The detrimental effect on the properties above these tempering temperatures is attributed to the fine carbide precipitation which promotes shear localization.

References

1. T. J. KOPPENAAL, *Trans. ASM* **62** (1969) 24.
2. D. J. LATHAM, *J. Iron Steel Inst.* **208** (1970) 50.
3. R. L. MILLER, *Trans. ASM* **61** (1968) 592.
4. Y. TOMITA, *J. Mater. Sci.* **24** (1989) 731.
5. C. J. BALL, *J. Iron Steel Inst.* **191** (1951) 232.
6. D. H. WARRINGTON, *ibid.* **201** (1963) 610.
7. J. D. BAIRD, *ibid.*, **204** (1966) 44.
8. R. L. JHONES and H. CANARD, *Trans. TMS-AIME*, **245** (1969) 779.
9. L. F. PORTER and D. S. DABKOWSKI, in Proceedings of the 16th Sagamore Army Materials Research Conference on "Ultrafine grain metals", edited by J. J. Burke and V. Weiss, (Syracuse University Press, New York 1969) p. 131.
10. W. M. MORRISON and R. L. MILLER, *ibid.* p. 183.
11. J. J. IRANI, *J. Iron Steel Inst.* **206** (1968) 363.
12. S. WATANABE, T. ARAKI, and H. MIYAJI, *J. Iron Steel Inst. Jpn.* **9** (1969) 792.
13. T. ARAKI, S. WATANABE, and H. MIYAJI, in "Toward improved ductility and toughness" (Climax Molybdenum Development Company Ltd., Kyoto, Japan, 1971) p. 171.
14. R. W. K. HONEYCOMBE in "The plastic deformation of metal" (Edward Arnord, London, 1968) p. 1203.

15. B. R. BANERJEE, *J. Iron Steel Inst.* **203** (1965) 166.
16. V. F. ZACKAY, E. R. GPARKER, R. D. GOOLSHY, and W. E. WOOD, *Natural Phys. Sci.* **236** (1972) 108.
17. E. R. PARKER and V. F. ZACKAY, *Eng. Fract. Mech.* **7** (1975) 371.
18. M. SARIKAYA, B. G. STEINBERG, and G. THOMAS, *Metall. Trans. A* **13A** (1982) 2227.
19. T. SIOYA, S. YAMADA, and Y. TARUTANI, *J. Metal Inst. Jpn.* **31** (1967) 126.
20. T. SIOYA, S. YAMADA, and S. INADA, *ibid.* **31** (1967) 347.
21. J. MaMAHON and G. THOMAS, in Proceedings of the 3rd International Conference on Strength of Metals and Alloys Vol. 1 (Inst. of Metals and the Iron and Steel Inst. London, 1973) p. 180.
22. S. K. DAS and G. THOMAS, *Trans. ASM* **62** (1969) 659.

Received 17 January
and accepted 16 May 1990